

Molecular Dynamics Simulation of Liquid Alkanes III. Thermodynamic, Structural, and Dynamic Properties of Branched-Chain Alkanes

Song Hi Lee*, Hong Lee, and Hyungsuk Pak †

Department of Chemistry, Kyungsoong University, Pusan 608-736, Korea

†Department of Chemistry, Seoul National University, Seoul 151-740, Korea

Received January 9, 1997

In recent papers [*Bull. Kor. Chem. Soc.* **1996**, *17*, 735; *ibid* **1997**, *18*, 478] we reported results of molecular dynamics (MD) simulations for the thermodynamic, structural, and dynamic properties of liquid normal alkanes, from *n*-butane to *n*-heptadecane, using three different models. Two of the three classes of models are collapsed atomic models while the third class is an atomistically detailed model. In the present paper we present results of MD simulations for the corresponding properties of liquid branched-chain alkanes using the same models. The thermodynamic property reflects that the intermolecular interactions become weaker as the shape of the molecule tends to approach that of a sphere and the surface area decreases with branching. Not like observed in the straight-chain alkanes, the structural properties of model III from the site-site radial distribution function, the distribution functions of the average end-to-end distance and the root-mean-squared radii of gyration are not much different from those of models I and II. The branching effect on the self diffusion of liquid alkanes is well predicted from our MD simulation results but not on the viscosity and thermal conductivity.

Introduction

In recent papers,^{1,2} we carried out equilibrium MD simulations of three different models for liquid normal alkanes (*n*-alkanes) to investigate the thermodynamic, structural and dynamic properties of liquid *n*-butane to *n*-heptadecane. In the present paper the same technique is applied to study the corresponding properties of branched-chain alkanes. Four different branched-chain alkanes are chosen: isobutane (*i*-butane), 4-propyl heptane (4-ph), 6-pentyl duodecane (6-pdd), and 5-dibutyl nonane (5-dbn) and the same three different molecular models as in the previous works^{1,2} are used for the branched-chain alkanes.

Normal butane (*n*-butane) and isobutane (*i*-butane) have the same molecular formula: C₄H₁₀. The two compounds have their atoms connected in a different order and are, therefore, constitutional isomers. Constitutional isomers have different physical properties. The differences may not always be large, but they will always be found to have different melting points, boiling points, densities, indexes of refraction, and so forth. For example, in every case a branched-chain isomer has a lower boiling point than a straight-chain isomer. Thus *n*-butane has a boiling point of 0 °C and *i*-butane – 12 °C, *n*-pentane has a boiling point of 36 °C, *i*-pentane with a single branch 28 °C, and neopentane with two branches 9.5 °C. This effect of branching on boiling point is observed within all families of organic compounds. That branching should lower the boiling point is reasonable: with branching the shape of the molecule tends to approach that of a sphere; and as this happens that the surface area decreases, with the result that the intermolecular forces become weaker and are overcome at a lower temperature.

The branching effect on the dynamic properties of liquid alkanes such as self diffusion coefficient, viscosity, and thermal conductivity is one of the most interesting phenomena of nowadays. For liquid butane, the experimentally ob-

served behaviour³ tells us that viscosity is found to increase with branching. However, for liquid pentane, hexane, and heptane, branching decreases the viscosity – 0.240 cP and 0.223 for *n*-pentane and *i*-pentane, 0.326 and 0.306 for *n*-hexane and *i*-hexane, and 0.409 and 0.384 for *n*-heptane and *i*-heptane,⁴ respectively.

To investigate the molecular cause of the structural branching effect upon viscosity, NEMD simulations of LJ site-site models representing *n*-butane and *i*-butane were performed over much of the density range for which experimental data are available, by Rowley and Ely.⁵ Simulated viscosities at zero shear agreed very well with experimental data over the entire density range. Site-size, non-equilibrium molecular alignment and molecular geometry were the primary factors causing both the similarities and differences between isomers' viscosity and rheology.

More recently, Lee and Cummings⁶ have reported an NEMD simulations of planar Couette flow of *n*-butane and *i*-butane molecules using the three different models.^{1,2} They found that the collapsed atomic models predict the viscosity of *n*-butane quite well in general agreement with previous workers^{5,7-8} but if these models are applied to the isomer, the viscosity is underpredicted. They also found that their atomistically detailed model does not yield quantitative agreement with the viscosity of either the *n*-butane or its isomer. However this model has the one positive feature that the calculated viscosity of *i*-butane is higher than that of *n*-butane (branching increases the viscosity) as observed experimentally. The results suggest that the inclusion of H atoms may be important in correctly predicting the effect of molecular structure on physical properties of liquid alkanes.

Unfortunately, the branching effect on the other two dynamic properties of liquid alkanes, self diffusion coefficient and thermal conductivity, is rarely reported in the literature, both experimentally and theoretically.

In this paper, we continue a series of molecular dynamics

simulation studies to investigate the thermodynamic, structural, and dynamic properties of liquid branched alkanes, *i*-butane, 4-propyl heptane, 6-pentyl duodecane, and 5-dibutyl nonane, using the three different molecular models used in the previous works.^{1,2} Further studies include analyses of segmental motions of C-C backbone chains in long chain alkanes.

The paper is organized as follows. Section II contains a brief description of molecular models and MD simulation methods followed by Sec. III which presents the results of our simulations and Sec. IV where our conclusions are summarized.

Molecular Dynamics Simulations and Molecular Models

Continuing the MD simulations of 14 liquid *n*-alkanes,^{1,2} we have chosen four branched-chain alkanes – isobutane (*i*-butane), 4-propyl heptane(4-ph), 6-pentyl duodecane (6-pdd), and 5-dibutyl nonane(5-dbn) to study the branching effect on thermodynamic, structural, and dynamic properties of liquid alkanes. The same three different molecular models as in the previous works^{1,2} are used for the branched-chain alkanes – the original RB collapsed atomic model (model I), the expanded collapsed atomic model (model II), and the atomistically detailed model (model III). The MD simulation parameters such as number of molecules, mass of site, temperature, and length of simulation box are listed in Table 1. The usual periodic boundary condition in the *x*-, *y*-, and *z*-directions and minimum image convention for pair potential

Table 1. MD simulation parameters for models of liquid branched-chain alkanes

Branched-chain alkane	Number of molecules	Mass of site* (g/mole)	Temperature (K)	Density (g/cc)	Length of box (nm)
<i>i</i> -butane	64	14.531	291.0	0.583	2.1964
4-ph	27	14.228	293.15	0.730	2.0598
6-pdd	27	14.145	296.0	0.782	2.3979
5-dbn	27	14.145	296.0	0.782	2.3979

*For model III, the masses of carbon and hydrogen atoms

Table 2. Thermodynamic properties of model I for liquid *i*-butane, 4-propyl heptane(4-ph), 6-pentyl duodecane(6-pdd), and 5-dibutyl nonane(5-dbn)

Properties	<i>i</i> -butane	4-ph	6-pdd	5-dbn
Molecular temperature (K)	291.0 ± 1.6	293.15 ± 1.56	296.0 ± 0.0	296.0 ± 0.0
Atomic temperature (K)	246.4 ± 12.2	253.05 ± 17.69	257.3 ± 8.2	264.7 ± 13.6
Pressure (atm)	301.4 ± 238.2	-210.9 ± 278.1	-441.7 ± 217.7	-285.8 ± 252.0
Total C-C LJ en. (kJ/mol)	-17.34 ± 0.29	-55.46 ± 0.82	-107.99 ± 0.66	-92.01 ± 0.92
Inter C-C LJ energy	-17.34 ± 0.29	-49.72 ± 0.67	-91.95 ± 0.54	-81.40 ± 0.73
Intra C-C LJ energy		-5.74 ± 0.24	-16.04 ± 0.05	-10.62 ± 0.38
C-C-C-C torsional energy		2.073 ± 0.104	2.066 ± 0.016	2.125 ± 0.063
Av. % of C-C-C-C trans		92.13 ± 5.05 ^a	77.48 ± 14.68 ^b	76.56 ± 23.85 ^c
Total barrier cross T-G		145/100,000	491/100,000	128/100,000
G-T		141/100,000	494/100,000	131/100,000
Av. end-to-end dist.(nm)	0.2498 ± 0.0048	0.6456 ± 0.0045	0.9676 ± 0.0008	0.7566 ± 0.0029
RMS radius of gyration	0.1267 ± 0.0018	0.2572 ± 0.0017	0.3926 ± 0.0031	0.3260 ± 0.0027

^aAverage of 3 dihedral states. ^bAverage of 10 dihedral states. ^cAverage of 8 dihedral states.

were applied. A spherical cut-off of radius $R_c=2.5\sigma$, where σ is the LJ parameter, was employed for all the pair interactions. Gaussian isokinetics⁹ was used to keep the temperature of the system constant.

Not like in the straight-chain alkanes, there are multiply imposed torsional rotational potentials in the branched-chain alkanes. For example, three doubly imposed dihedral states on the bonds of 3-4, 4-5, and 4-8 in 4-ph, and on those of 5-6, 6-7, and 6-13 in 6-pdd, and four triply imposed dihedral states on the bonds of 4-5, 5-6, 5-13, and 5-14 in 5-dbn exist as shown in Figure 1. These multiply imposed torsional rotational potentials are assumed to be equal to the sum of torsional rotational potential of each dihedral state.

Results and Discussion

In this section we analyze the results of our MD simulations; the principal thermodynamic, structural, and dynamic properties of branched-chain alkanes are considered

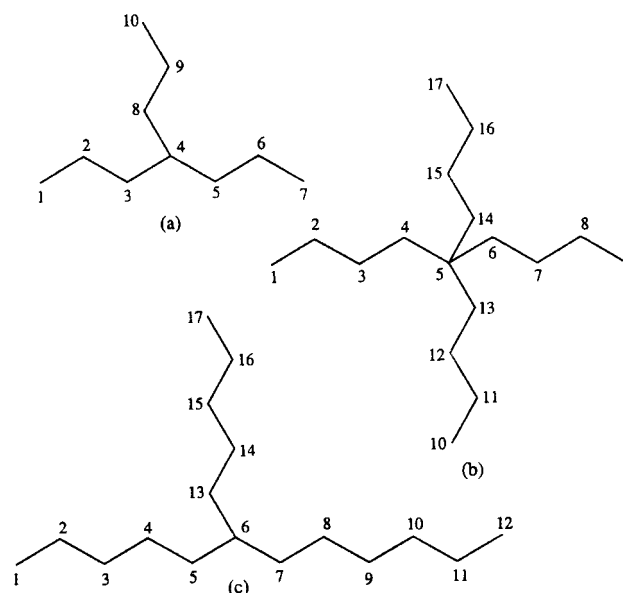


Figure 1. Geometries of (a) 4-propyl heptane(4-ph), (b) 6-pentyl duodecane(6-pdd), and (c) 5-dibutyl nonane(5-dbn).

Table 3. Thermodynamic properties of model II for liquid *i*-butane, 4-propyl heptane(4-ph), 6-pentyl duodecane(6-pdd), and 5-dibutyl nonane(5-dbn)

Properties	<i>i</i> -butane	4-ph	6-pdd	5-dbn
Molecular temperature (K)	291.0 ± 0.4	293.15 ± 0.009	296.0 ± 0.5	296.0 ± 0.5
Atomic temperature (K)	268.2 ± 26.3	264.72 ± 30.07	263.3 ± 29.6	254.8 ± 31.3
Pressure (atm)	379.3 ± 281.7	-154.3 ± 393.6	-258.3 ± 380.9	-440.8 ± 375.2
Total C-C LJ en. (kJ/mol)	-17.25 ± 0.36	-54.25 ± 0.96	-107.61 ± 1.45	-90.87 ± 1.43
Inter C-C LJ energy	-17.25 ± 0.36	-44.22 ± 0.67	-76.18 ± 0.54	-68.46 ± 0.73
Intra C-C LJ energy	-	-10.23 ± 0.66	-31.43 ± 0.50	-22.41 ± 1.51
C-C-C torsional energy	-	2.423 ± 0.166	2.167 ± 0.161	2.192 ± 0.119
C-C stretching energy	1.565 ± 0.159	8.048 ± 1.137	13.50 ± 1.82	16.68 ± 2.06
C-C-C angle bend energy	3.674 ± 0.420	10.11 ± 1.47	18.02 ± 2.26	20.42 ± 2.58
Av. % of C-C-C trans	-	91.55 ± 3.03 ^a	78.81 ± 8.59 ^b	80.48 ± 19.68 ^c
Total barrier cross T-G	-	176/100,000	577/100,000	296/100,000
G-T	-	177/100,000	579/100,000	299/100,000
Av. end-to-end dist.(nm)	0.2501 ± 0.0008	0.6459 ± 0.0066	1.0068 ± 0.0190	0.6551 ± 0.0138
RMS radius of gyration	0.1270 ± 0.0008	0.2556 ± 0.0023	0.4032 ± 0.0075	0.3306 ± 0.0044

^a Average of 3 dihedral states. ^b Average of 10 dihedral states. ^c Average of 8 dihedral states.

Table 4. Thermodynamic properties of model III for liquid *i*-butane, 4-propyl heptane(4-ph), 6-pentyl duodecane(6-pdd), and 5-dibutyl nonane(5-dbn)

Properties	<i>i</i> -butane	4-ph	6-pdd	5-dbn
Molecular temperature (K)	291.0 ± 0.1	293.15 ± 0.18	296.0 ± 0.3	296.0 ± 0.3
Atomic temperature (K)	264.3 ± 22.3	327.81 ± 44.0	310.3 ± 40.1	302.4 ± 33.9
Pressure (atm)	61.3 ± 374.9	-274.8 ± 571.4	-150.5 ± 479.1	-262.6 ± 457.0
Total C-C LJ en. (kJ/mol)	-15.56 ± 0.43	-42.33 ± 1.21	-78.63 ± 1.37	-73.82 ± 1.52
Inter C-C LJ energy	-7.08 ± 0.17	-18.79 ± 0.40	-35.92 ± 0.46	-30.70 ± 0.42
Inter C-H LJ energy	-6.95 ± 0.21	-16.88 ± 0.44	-30.83 ± 0.50	-27.26 ± 0.48
Inter H-H LJ energy	-0.84 ± 0.17	-3.22 ± 0.84	-2.23 ± 0.654	-2.52 ± 0.55
Intra C-C LJ energy	-	-2.73 ± 0.10	-5.43 ± 0.163	-9.12 ± 0.10
Intra C-H LJ energy	-	-0.97 ± 0.34	-3.51 ± 0.364	-4.48 ± 0.52
Intra H-H LJ energy	-0.69 ± 0.02	0.26 ± 0.34	-0.71 ± 0.391	0.26 ± 0.47
C-C-C torsional energy	-	2.340 ± 0.242	2.392 ± 0.189	2.411 ± 0.120
C-C-C-H torsional energy	1.398 ± 0.186	1.396 ± 0.331	1.467 ± 0.263	1.364 ± 0.257
C-C stretching energy	4.589 ± 0.528	12.34 ± 1.97	20.40 ± 3.10	20.19 ± 2.54
C-H stretching energy	18.26 ± 1.38	31.65 ± 4.834	49.08 ± 6.69	47.88 ± 5.87
C-C-C angle bend energy	3.328 ± 0.404	10.20 ± 1.56	16.86 ± 2.21	20.57 ± 2.19
C-C-H angle bending energy	11.63 ± 1.03	16.95 ± 2.37	23.45 ± 3.51	25.50 ± 3.01
H-C-H angle bending energy	15.17 ± 1.06	40.87 ± 5.78	67.79 ± 9.38	61.08 ± 7.13
Av. % of C-C-C trans	-	79.13 ± 8.42 ^a	75.73 ± 12.89 ^b	81.82 ± 16.10 ^c
Total barrier cross T-G	-	296/100,000	783/100,000	833/100,000
G-T	-	294/100,000	779/100,000	828/100,000
Av. end-to-end dist.(nm)	0.2509 ± 0.0007	0.6387 ± 0.0073	1.0862 ± 0.0184	0.6978 ± 0.0103
RMS radius of gyration	0.1273 ± 0.0011	0.2608 ± 0.0049	0.4110 ± 0.0032	0.3368 ± 0.0038

^a Average of 3 dihedral states. ^b Average of 10 dihedral states. ^c Average of 8 dihedral states.

separately.

Thermodynamic properties. Thermodynamic properties of models I, II, and III for liquid isobutane (*i*-butane), 4-propyl heptane(4-ph), 6-pentyl duodecane(6-pdd), and 5-dibutyl nonane(5-dbn) are listed in Tables 2, 3, and 4, respectively. Comparing with the corresponding properties of models for *n*-alkanes, the total C-C LJ energies are almost the same except 5-dbn, but the inter C-C LJ energies are negatively much less than those in *n*-alkanes which reflects that the intermolecular interactions become weaker as the shape of the molecule tends to approach that of a sphere and the surface area decreases with branching.

Another branching effect on the thermodynamic property is the large increment of the C-C and C-H bond stretching, and the C-C-C, C-C-H and H-C-H angle bending potential energies. This effect is especially large in the case of 5-dbn. As the shape of the molecule tends to approach that of a sphere, the steric effect becomes larger and the monomeric units repel each other, which contributes the large repulsive interactions of the bond stretching and the bond angle bending potential energies.

In contrast to 7 dihedral states in *n*-decane, there are 9 dihedral states in 4-ph as shown Figure 1(a): 1-2-3-4, 2-3-4-5, 3-4-5-6, 4-5-6-7, 4-8-9-10, 2-3-4-8, 3-4-8-9, 5-4-8-9, and

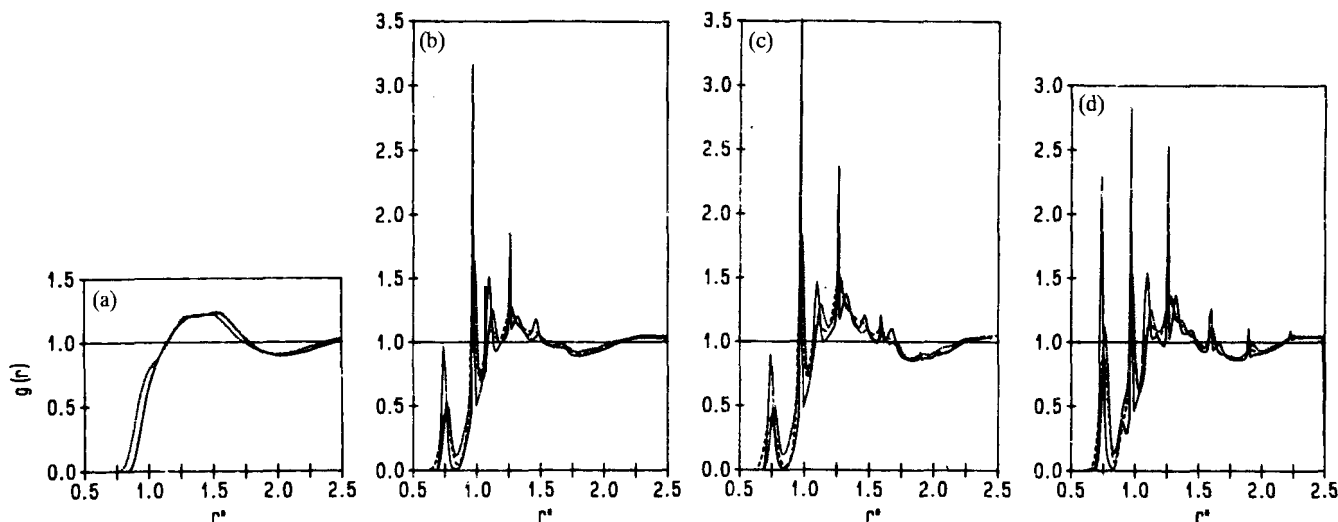


Figure 2. Site-site radial distribution functions of models I(—), II(---), and III(···) for liquid branched-chain alkanes, $r^* = r/\sigma$. (a) *i*-butane, (b) 4-propyl heptane, (c) 6-pentyl duodecane, and (d) 5-dibutyl nonane.

8-4-5-6. Because of doubly imposed torsional rotational potentials on the bonds of 3-4, 4-5, and 4-8, the dihedral states of 2-3-4-5, 3-4-5-6, 2-3-4-8, 3-4-8-9, 5-4-8-9, and 8-4-5-6 are almost fixed and so only three dihedral states of 1-2-3-4, 4-5-6-7, and 4-8-9-10 are subject to the usual torsional rotational potentials. The average % of C-C-C-C trans and the total barrier cross T-G and G-T of model I, II, and III for 4-ph in Tables 2, 3, and 4 are for the three dihedral states but the average C-C-C-C torsional energy per dihedral state is obtained from the whole dihedral states.

Similarly, in contrast to 14 dihedral states in *n*-heptadecane, there are 20 and 16 dihedral states in 5-dbn and 6-pdd, respectively, as shown Figures 1(b) and (c). Because of doubly and triply imposed torsional rotational potentials on the bonds of the branched-chain alkanes (6-pdd and 5-dbn), the 6 dihedral states of 6-pdd and 12 dihedral states of 5-dbn are almost fixed and so only 10 dihedral states of 6-pdd and 8 dihedral states of 5-dbn are subject to the usual torsional rotational potentials. The average % of C-C-C-C trans of model I, II, and III for branched-chain alkanes are generally much increased and the total barrier crossings T-G and G-T are largely decreased in comparing with the straight-chain alkanes. This is also one of the results of the branching effect which reflects that as the shape of the molecule tends to approach that of a sphere, the steric effect becomes larger, the chains tend to straighten up, and the dihedral states are almost fixed due to the repulsive forces between monomers. But in model III the intra bond stretching and bond angle bending potentials may overcome the high barrier crossing energy.

Structural properties. The site-site radial distribution functions, $g(r)$, of models I, II, and III for liquid branched-chain alkanes are shown in Figure 2. The whole trend of $g(r)$ for branched-chain alkanes, Figure 2(a), is slightly different from that of straight-chain alkanes, Figure 4(h) in Ref. 1, in view of the plateau at $r^* = 1.25 \sim 1.6$. The $g(r)$ functions of the three different models are almost the same except shifts to the smaller r^* at $r^* = 0.75 \sim 1.1$ and $1.6 \sim 1.75$.

In Figures 2(b), (c), and (d), the $g(r)$ functions of 4-ph, 6-

pdd, and 5-dbn show the sharp peaks correspond to gauche (G) and trans (T), and to the contributions of TT, TTT, TTTT, and TTTTT at $r^* = 1.27, 1.61, 1.91,$ and 2.24 , respectively. Between these sharp peaks, there are somewhat broad curves correspond to the contributions of TG between T and TT, TTG and TGT between TT and TTT, and TTTG (or equivalently TGTG) between TTT and TTTT at $r^* = 1.1, 1.3, 1.45,$ and 1.8 , respectively. The difference between Figures 2(b) and (c) is very little except the contributions of TTT and TTTG (or TGTG) as expected for the geometries of 4-ph and 6-pdd in Figure 1. The relatively larger peak of G in the $g(r)$ of 5-dbn in Figure 2(d) than those of 4-ph and 6-pdd in Figures 2(b) and (c) is due to the branching effect on the structural property – two branches vs. a single branch. It is worth noting that the structural properties of model III from $g(r)$ are not much different from those of models I and II in view of Figures 2(a), (b), (c), and (d).

In Figures 3 and 4, we have shown the distribution functions of the average end-to-end distance and the root-mean-squared radii of gyration of models I, II, and III for liquid branched-chain alkanes as a function of r^* . There is no contribution corresponds to gauche (G) and trans (T) in the case of *i*-butane and both functions for *i*-butane, "i" in Figures 3 and 4, show a delta function with sharp peak of model I and broad peaks of models II and III due to the bond stretching and bond angle bending potentials.

In the case of 4-ph, two distinct peaks of the average end-to-end distance and the root-mean-squared radii of gyration of model I become weakened in Models II and III, while in the case of 5-dbn, three distinct peaks of the average end-to-end distance do not disappear in models I, II, and III but four distinct peaks of the root-mean-squared radii of gyration of model I become weakened in Models II and III. On the other hand, both functions of models I, II, and III for 6-pdd are all smooth broad curves. Not like observed in the straight-chain alkanes, the structural properties of model III from the distribution functions of the average end-to-end distance and the root-mean-squared radii of gyration are not much different from those of models I and II.

Dynamic Properties. The mean square displacements

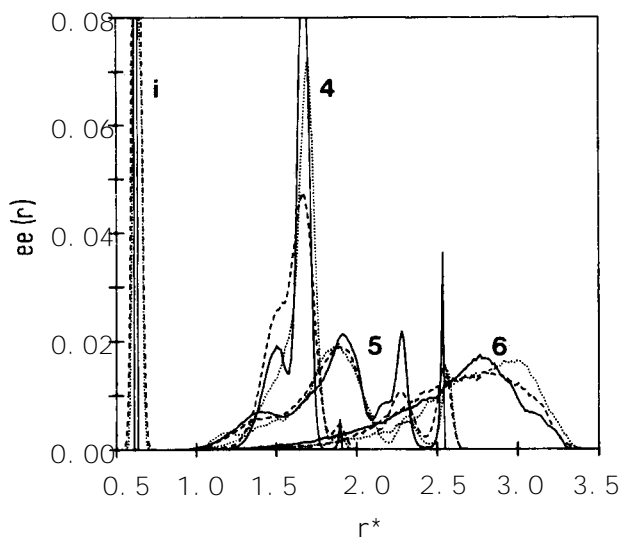


Figure 3. Average end-to-end distance distribution of models I (—), II(---), and III(⋯) for liquid branched-chain alkanes, $r^* = r/\sigma$. (i) *i*-butane, (4) 4-propyl heptane, (6) 6-pentyl duodecane, and (5) 5-dibutyl nonane.

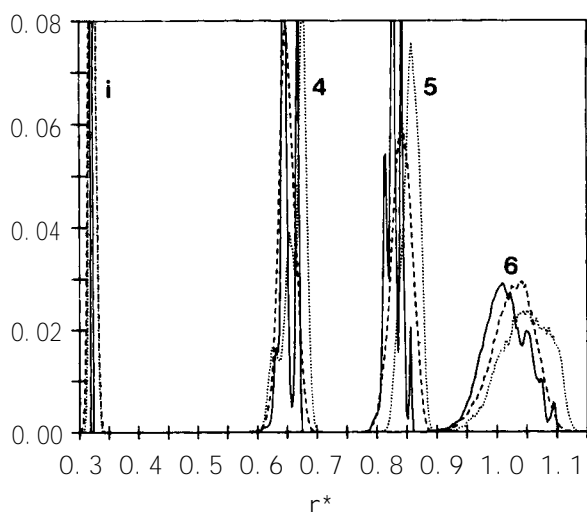


Figure 4. Root-mean-squared radius of gyration distribution of models I(—), II(---), and III(⋯) for liquid branched-chain alkanes, $r^* = r/\sigma$. (i) *i*-butane, (4) 4-propyl heptane, (6) 6-pentyl duodecane, and (5) 5-dibutyl nonane.

(MSD) and normalized velocity auto-correlation (VAC) functions of liquid branched-chain alkanes are shown in Figures 5 and 6, respectively. The self diffusion coefficients of models I, II, and III for liquid branched-chain alkanes calculated from MSD's using the Einstein equation:

$$D_s = \frac{1}{6} \lim_{t \rightarrow \infty} \frac{d \langle |r(t) - r(0)|^2 \rangle}{dt} \quad (1)$$

are listed in Table 5. The calculated self diffusion coefficient from MSD from our MD simulation decreases as the branching is increased except model I of *n*-butane and *i*-butane, and *n*-decane and 4-ph. This is the branching effect on the self diffusion property of liquid alkanes.

The normalized VAC of model II for all the branched-chain alkanes show very different trends from those of the

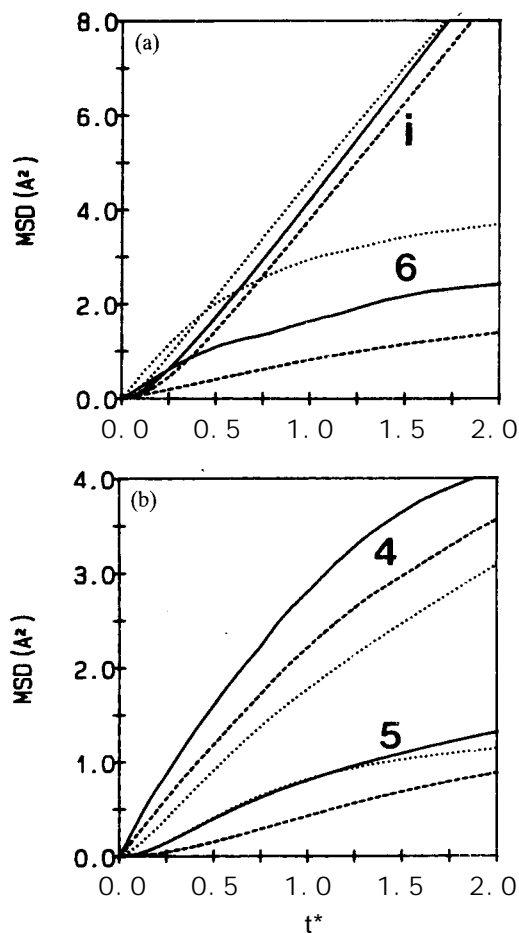


Figure 5. Mean square displacements of models I(—), II(---), and III(⋯) for liquid branched-chain alkanes with t^* in ps. (a) *i*-butane(i) and 6-pentyl duodecane(6), (b) 4-propyl heptane(4) and 5-dibutyl nonane(5).

other two models in Figure 6. The self diffusion coefficients of model II for all the branched-chain alkanes calculated from the VAC's using the Green-Kubo relations¹⁰ give somewhat strange results as shown in Table 6. As discussed in Ref. 2, the self diffusion coefficient can be separated into two parts according to:

$$D_s = \frac{1}{3} \int_0^\infty \langle v(0) \cdot v(t) \rangle dt = \frac{kT}{m} A \quad (2)$$

where v is the velocity of particle, since $m \langle v(0) \cdot v(0) \rangle = mv^2 = 3kT$ and

$$A = \int_0^\infty \frac{\langle v(0) \cdot v(\tau) \rangle}{\langle v(0) \cdot v(0) \rangle} d\tau. \quad (3)$$

The integration values of the normalized VAC functions of model II for all the branched-chain alkanes are too large but the calculated values of kT/m are usual as seen in Table 6. Except the self diffusion coefficients of model II for all the branched-chain alkanes calculated from the VAC's, the calculated self diffusion coefficient from VAC from our MD simulation also decreases as the branching is increased. Hence the branching effect on the self diffusion property of liquid alkanes is confirmed.

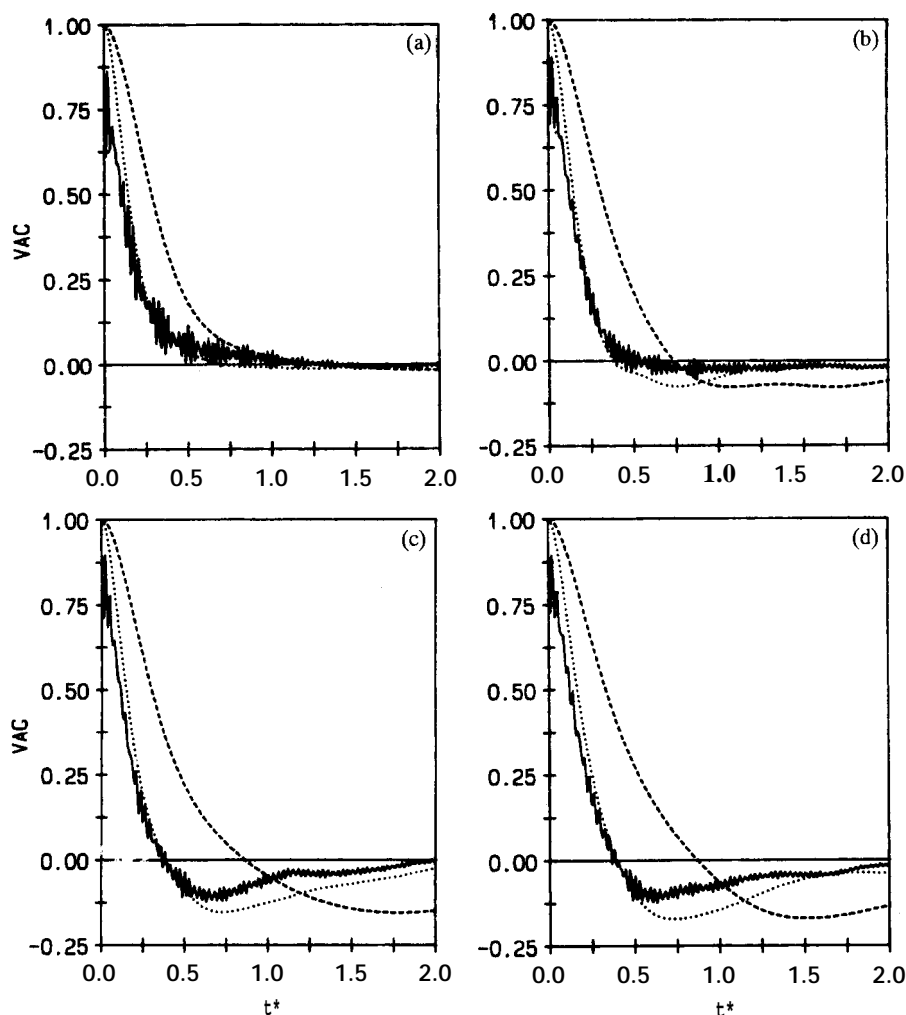


Figure 6. Normalized velocity auto-correlation functions of models I(—), II(---), and III(···) for liquid branched-chain alkanes with t^* in ps. (a) *i*-butane, (b) 4-propyl heptane, (c) 6-pentyl duodecane, and (d) 5-dibutyl nonane.

Table 5. Self diffusion coefficients(D_s , 10^9 m²/s) of model II for liquid *i*-butane, 4-propyl heptane(4-ph), 6-pentyl duodecane(6-pdd), and 5-dibutyl nonane(5-dbn) calculated from MSD using Eq. (1)

Alkane	D_s	Alkane	D_s
<i>i</i> -butane	3.54 (7.96) ^a [8.58] ^b	4-ph	2.61 (2.37) ^a [5.16] ^b
6-pdd	1.10 (1.942) ^a [1.598] ^b	5-dbn	0.833 (0.689) ^a [0.994] ^b

^aModel I, ^bModel III.

The normalized stress auto-correlation (SAC) and heat-flux auto-correlation (HFAC) functions of models I, II and III for liquid branched-chain alkanes are shown in Figures 7 and 8, respectively. Both functions of model II of all the branched-chain alkanes also show a different behavior from those of the other two models. As discussed in Sec. I, the branching effect on the viscosity property of liquid alkanes is that branching decreases the viscosity. However, unfortunately there is no experimental data available for the

Table 6. Self diffusion coefficients(D_s , 10^9 m²/s) of model II for liquid *i*-butane, 4-propyl heptane(4-ph), 6-pentyl duodecane(6-pdd), and 5-dibutyl nonane(5-dbn) calculated from SAC. A (ps) is the value of Eq. (3) and kT/m in 10^3 m²/s²

Alkane	kT/m	A	D_s
<i>i</i> -butane	42.11 (41.49) [44.92]	0.3319 0.1732 0.1923	13.98 7.19) ^a 8.64] ^b
4-ph	16.43 (15.81) [16.81]	0.3093 0.1262 0.1537	5.08 2.00) ^a 2.58] ^b
6-pdd	9.699 (9.328) [9.847]	0.2765 0.0762 0.0941	2.68 0.711) ^a 0.923] ^b
5-dbn	9.700 (9.334) [9.775]	0.2837 0.0820 0.0941	2.75 0.765) ^a 0.927] ^b

^aModel I, ^bModel III and in the calculation of D_s , the mass of C atoms only is considered.

branching effect on the thermal conductivity of liquid alkanes.

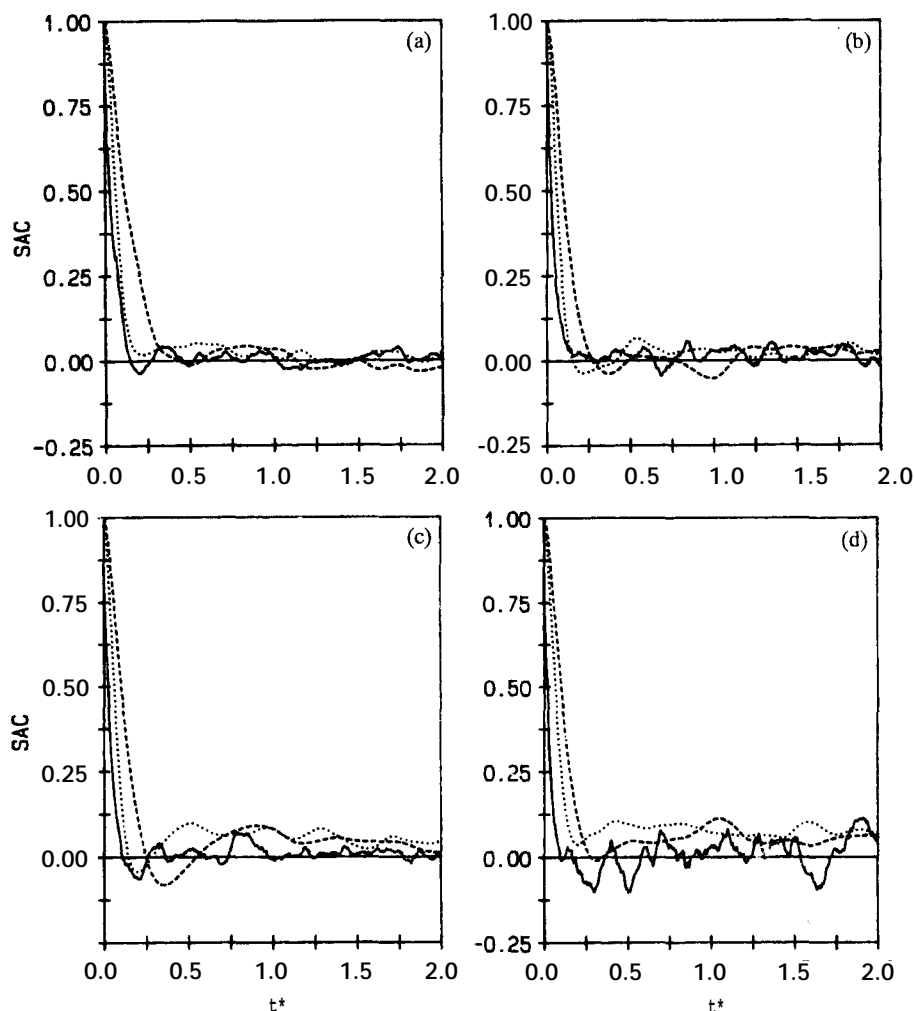


Figure 7. Normalized stress auto-correlation functions of models I(—), II(---), and III(⋯) for liquid branched-chain alkanes with t^* in ps. (a) *i*-butane, (b) 4-propyl heptane, (c) 6-pentyl duodecane, and (d) 5-dibutyl nonane.

The calculated viscosities and thermal conductivities of models I, II, and III for branched-chain alkanes from the Green-Kubo relations¹⁰ are listed in Tables 7 and 8, respectively. Those values are again separated into two parts according to:

$$\eta = \frac{V}{kT} \int_0^{\infty} \langle P_{xy}(0) \cdot P_{xy}(t) \rangle dt$$

$$= \frac{V \langle P_{xy}^2 \rangle}{kT} B \quad (4)$$

where P_{xy} is an off-diagonal ($x \neq y$) of the viscous pressure tensor,

$$PV = \sum_{i=1}^N m v_i v_i + \sum_{i=1}^N r_i F_i \quad (5)$$

$$\text{and} \quad B = \int_0^{\infty} \frac{\langle P_{xy}(0) \cdot P_{xy}(\tau) \rangle}{\langle P_{xy}(0) \cdot P_{xy}(0) \rangle} d\tau \quad (6)$$

$$\text{And} \quad \lambda = \frac{1}{kT^2} \int_0^{\infty} \langle J_{Qx}(t) \cdot J_{Qx}(0) \rangle dt$$

$$= \frac{V \langle J_{Qx}^2 \rangle}{kT^2} C \quad (7)$$

where J_{Qx} is a component of the energy current vector, J_Q

$$J_Q V = \sum_{i=1}^N E_i v_i - \frac{1}{2} \sum_i \sum_j r_{ij} (v_i \cdot F_{ij}) \quad (8)$$

$$\text{and} \quad C = \int_0^{\infty} \frac{\langle J_{Qx}(0) \cdot J_{Qx}(\tau) \rangle}{\langle J_{Qx}(0) \cdot J_{Qx}(0) \rangle} d\tau \quad (9)$$

The calculated viscosities and thermal conductivities from SAC and HFAC from our MD simulation are too much varied to predict the branching effect on the viscosity and thermal conductivity of liquid alkanes. The variation of our MD simulation results for the viscosities and thermal conductivities of liquid branched-chain alkanes may be possibly involved in several aspects, but the most significant point is due to the limitation of equilibrium MD simulation using Green-Kubo relations for the thermal transport properties of liquid branched-chain alkanes, and that explains why the non-equilibrium MD simulation has been developed recently

Conclusions

We have carried out a series of MD simulations of liquid alkanes using three different models. In a recent paper,¹ we reported the MD simulation results for the thermodynamic

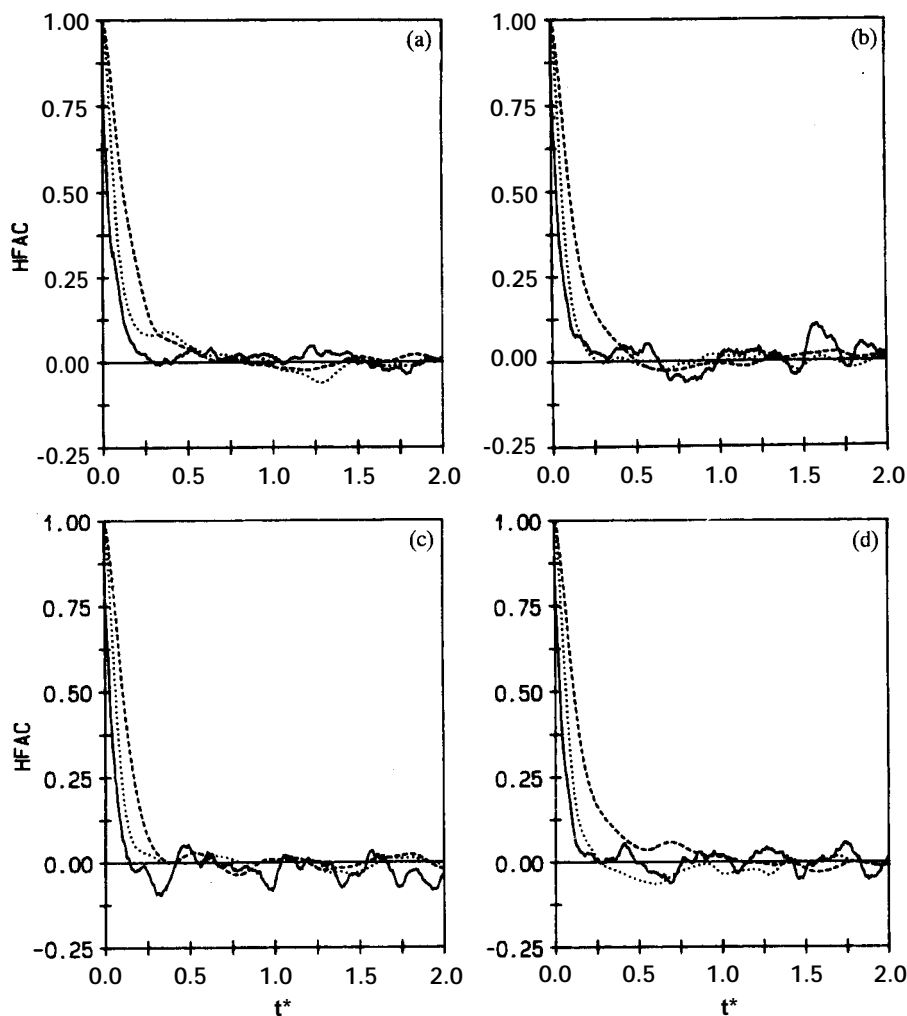


Figure 8. Normalized heat-flux auto-correlation functions of models I(—), II(---), and III(⋯) for liquid branched-chain alkanes with t^* in ps. (a) *i*-butane, (b) 4-propyl heptane, (c) 6-pentyl duodecane, and (d) 5-dibutyl nonane.

Table 7. Viscosities (η , cP) of model II for liquid *i*-butane, 4-propyl heptane(4-ph), 6-pentyl duodecane(6-pdd), and 5-dibutyl nonane(5-dbn) calculated from SAC. B (ps) is the value of Eq. (6) and $V\langle p_v^2 \rangle / kT$ in cP/ps

Alkane	$V\langle p_v^2 \rangle / kT$	B	η
<i>i</i> -butane	1.470	0.1642	0.219
	(1.448)	0.1056	0.153) ^a
	[2.354	0.05007	0.118] ^b
4-ph	3.496	0.1103	0.386
	(3.337)	0.08180	0.273) ^a
	[5.538	0.05416	0.300] ^b
6-pdd	6.858	0.1330	0.612
	(5.885)	0.09555	0.562) ^a
	[10.24	0.04063	0.416] ^b
5-dbn	5.049	0.1558	0.787
	(5.841)	0.1521	0.888) ^a
	[8.415	0.04811	0.505] ^b

^aModel I, ^bModel III and in the calculation of η , the mass of C atoms only is considered.

Table 8. Thermal conductivities (λ , J/s · m · K ps) for liquid *i*-butane, 4-propyl heptane(4-ph), 6-pentyl duodecane(6-pdd), and 5-dibutyl nonane(5-dbn) calculated from HFAC. C (ps) is the value of Eq. (9) and $V\langle J_q^2 \rangle / kT^2$ in J/s · m · K ps

Alkane	$V\langle J_q^2 \rangle / kT^2$	C	λ
<i>i</i> -butane	0.5159	0.1575	0.0813
	(0.5016)	0.1081	0.0542) ^a
	[0.7201	0.06864	0.0494] ^b
4-ph	0.4247	0.1364	0.0583
	(0.3729)	0.07541	0.0281) ^a
	[0.5825	0.03185	0.0348] ^b
6-pdd	0.4216	0.1228	0.0518
	(0.3473)	0.07763	0.0270) ^a
	[0.6281	0.04922	0.0309] ^b
5-dbn	0.3347	0.1663	0.0557
	(0.4106)	0.08052	0.0331) ^a
	[0.5515	0.04718	0.0260] ^b

^aModel I, ^bModel III and in the calculation of λ , the mass of C atoms only is considered.

and structural properties of liquid *n*-alkanes. Excellent agreement of the results of model I for *n*-butane from different

MD algorithms, ours and those of Edberg *et al.*,¹¹ confirmed the validity of our whole set of MD simulations of

model II for 14 liquid *n*- alkanes and of models I and III for liquid *n*- butane, *n*- decane, and *n*- heptadecane. The thermodynamic and structural properties of model I and II were very similar to each other and the thermodynamic properties of model III for the three *n*- alkanes are not much different from those of models I and II. However, the structural properties of model III were very different from those of model I and II as seen from the radial distribution functions, the average end-to-end distances, and the root-mean-squared radii of gyration.

In a more recent paper,² we reported the results of MD simulations for the dynamic properties of liquid *n*- alkanes using the same models. The agreement of two self-diffusion coefficients of liquid *n*- alkanes calculated from the MSD's via the Einstein equation and the VAC functions via the Green-Kubo relation was excellent. The viscosities of *n*-butane to *n*- nonane calculated from the SAC functions and the thermal conductivities of *n*- pentane to *n*- decane calculated from the HFAC functions via the Green-Kubo relations were smaller than the experimental values by approximately a factor of 2 and 4, respectively.

In the present paper, we report results of thermodynamic, structural, and dynamic properties from MD simulation of liquid branched-chain alkanes using the same models. The thermodynamic property reflects that the intermolecular interactions become weaker as the shape of the molecule tends to approach that of a sphere and the surface area decreases with branching. Not like observed in the straight-chain alkanes, the structural properties of model III from the site-site radial distribution function and the distribution functions of the average end-to-end distance and the root-mean-squared radii of gyration are not much different from those of models I and II. The branching effect on the self diffusion of liquid alkanes is well predicted but not on the

viscosity and thermal conductivity from our MD simulation.

Acknowledgments. This work was supported by Basic Science Research Institute Program, Ministry of Education (BSRI-95-3414). S. H. L. thanks the Korea Institute of Sciences and Technology for access to the Cray-C90 super computer.

References

1. Lee, S. H.; Lee, H.; Pak, H.; Rasaiah, J. C. *Bull. Kor. Chem. Phys.* **1996**, *17*, 735.
2. Lee, S. H.; Lee, H.; Pak, H. *Bull. Kor. Chem. Phys.* **1997**, *18*, 478.
3. Diner, D. E.; Van Poolen, L. J. *Int. J. Thermophys.* **1985**, *6*, 43.
4. Weast, R. C.; Astle, M. J. *CRC Handbook of Chemistry and Physics*, 63rd ed.; CRC press: Boca Ranton; 1982~1983.
5. Rowley, R. L.; Ely, J. F. *Mol. Phys.* **1991**, *72*, 831.
6. Lee, S. H.; Cummings, P. T. *Mol. Sim.* **1996**, *16*, 229.
7. Chynoweth, S.; Klomp, U. C.; Scales, L. E. *Comput. Phys. Commun.* **1991**, *62*, 297.
8. Edberg, R.; Morriss, G. P.; Evans, D. J. *J. Chem. Phys.* **1987**, *86*, 4555.
9. Evans, D. J.; Hoover, W. G.; Failor, B. H.; Moran, B.; Ladd, A. J. C. *Phys. Rev.* **1983**, *A28*, 1016. (b) Simmons, A. D.; Cummings, P. T. *Chem. Phys. Lett.* **1986**, *129*, 92.
10. (a) Green, M. S. *J. Chem. Phys.* **1951**, *19*, 249. (b) *ibid.* **1952**, *20*, 1281. (c) *ibid.* **1954**, *22*, 398. (d) Kubo, R. J. *Phys. Soc. Japan* **1957**, *12*, 570.
11. Edberg, R.; Evans, D. J.; Morriss, G. P. *J. Chem. Phys.* **1986**, *84*, 6933.